ELSEVIER

Journal of Molecular Catalysis A: Chemical 153 (2000) 129–137

JOURNAL OF MOLECULAR CATALYSIS A: CHEMICAL

www.elsevier.com/locate/molcata

Photochemical transformations of sodium anthracene-1-sulfonate in oxygen-saturated aqueous titanium dioxide suspensions

Alžbeta Blažková, Bronislava Mezeiová, Vlasta Brezová *, Michal Čeppan, Viera Jančovičová

Faculty of Chemical Technology, Slovak Technical University, Radlinského 9, SK-812 37 Bratislava, Slovak Republic

Received 19 April 1999; accepted 9 August 1999

Abstract

The decomposition of sodium anthracene-1-sulfonate (AN1S) by irradiation ($\lambda > 300$ nm) was investigated in oxygen-saturated aqueous solutions and TiO_2 suspensions. The concentration decrease of AN1S during exposure follows the formal first-order kinetics. The formation of phthalic and salicylic acids was monitored by high performance liquid chromatography (HPLC) in both photosystems. Additionally, the formation of alizarin during irradiation in the presence of TiO_2 was confirmed. The effect of experimental conditions (initial AN1S concentration, pH value, TiO_2 concentration) on the formal initial rate of AN1S photodegradation was studied in details. In situ EPR spin trapping experiments in TiO_2 suspensions confirmed the competitive reaction of photogenerated hydroxyl radicals between 5,5-dimethyl-1-pyrroline *N*-oxide (DMPO) spin trap and AN1S.

Keywords: Sodium anthracene-1-sulfonate; Phototransformation; Photocatalysis; TiO_2; EPR spin trapping

1. Introduction

The photochemical processes of waste water treatment represent alternative possibilities for the removal of organic and inorganic contamination from the aquatic environment [1–3]. The photocatalytic methods of pollutant destruction using powdered semiconductor or immobilized photocatalysts (TiO_2, ZnO, CdS, ...) were shown to be very efficient in the decomposition of phenols [3–6], halogenated compounds [3–5,7], surfactants [8–11], pesticides [12–14], etc. [1–3,15,16]. Due to the effective formation of hydroxyl radicals, hydrogen peroxide, and other reactive oxygen intermediates [2], strongly oxidizing conditions are generated in the irradiated oxygenated TiO_2 suspensions, enabling finally the total mineralization of organic compounds [2,3].

The systematic investigations of photocatalytic degradation of surfactants containing sulfonate groups [8–11] and sulfonated aromatics [17] in TiO_2 systems, confirmed the influence of substrate structures, and also experimental

* Corresponding author. Fax: +421-7-52493198; e-mail: brezova@cvtstu.cvt.stuba.sk

1381-1169/00/$ - see front matter
PII: S1381-1169(99)00312-X

conditions applied on the destruction rate [9,10,19]. However, only limited information is available on the photocatalytic degradation of sulfonated polycondensed aromatic compounds [4,5,20–22], although such structures are widely utilized in industrial dyes [23]. The photocatalytic transformations of naphthalene [4,5,20–22] and anthracene [22] in the aqueous TiO_2 suspensions were published. Phthalic acid and 9,10-anthraquinone were found to be the main intermediates in the degradation of anthracene [22].

Previously, in the EPR study of UV irradiated aqueous oxygen-saturated solutions of sodium anthracene-1-sulfonate (AN1S), employing the spin trapping technique, we confirmed the formation of intermediate anthracene-1-sulfonyl radical, as well as the generation of hydroxyl radicals [24]. Now, in the presented paper we compare the photochemical transformations of AN1S in the presence of oxygen, in homogeneous aqueous solutions and, additionally, in TiO_2 suspensions.

2. Experimental

2.1. Materials

Sodium AN1S (purity over 99.99%) was prepared and purified at the Department of Organic Chemistry, Faculty of Chemical Technology, Bratislava, Slovak Republic. Methanol (for chromatography), ethanol (spectroscopic grade), sodium hydroxide, phosphoric acid, sulfuric acid and $BaCl_2$ (all of analytical grade) were purchased from Lachema (Czech Republic), and were used without further purification. Perchloric acid from Laborchemie (Germany) and standard buffer solutions with pH values of 4.0 and 7.0 from Lovibond (Germany), were applied. Titanium dioxide powder P25 Degussa (Germany), characterized by the ratio anatase/rutile $\sim 70/30$, and surface area of 50 ± 5 m^2 g^{-1} [2] was used in the heterogeneous photochemical systems. Deionized and redistilled water was used for the solutions and suspensions preparation. The spin trap, 5,5-dimethyl-1-pyrroline *N*-oxide, (DMPO) (Sigma), was freshly distilled before use (75°C and 0.5 Torr) and stored at -25°C under argon. Ferrioxalate was synthesized at the Department of Printing Technology and Applied Photochemistry, Faculty of Chemical Technology, Bratislava, Slovak Republic.

2.2. Methods and apparatus

The samples were irradiated in a quartz cell (1-cm path length) using apparatus with the focused light beam of a 400-W medium-pressure mercury lamp (RUK, Holešovice, Czech Republic). A Pyrex filter was used to cut-off the radiation below 300 nm. The prepared aqueous solutions and suspensions were continuously bubbled by oxygen, 15 min before irradiation, and also during exposure the slight stream of oxygen was introduced into the cell. All photochemical experiments were performed at temperature of 295 K. The initial pH values of solutions and suspensions were adjusted by 0.5 M $HClO_4$ and 0.1 M NaOH addition.

The source light flux ($\Phi_0 = 1.1 \times 10^{-7}$ mol s^{-1}, corresponding to the light intensity of 0.01 W cm^{-2}) was determined by a standard procedure using ferrioxalate actinometer [25]. The monochromatic light with $\lambda = 365$ nm was selected by a filter (Schott Glaswerke, Germany) in the actinometry experiments.

The concentrations of AN1S and its degradation products in the irradiated samples were determined by the high performance liquid chromatography (FPLC Pharmacia, Sweden) using Separon SIX C-18 column (Tessek, Czech Republic) and UV detector ($\lambda = 280$ nm). A mixture of methanol–water (15:85) was applied as a mobile phase.

The UV/VIS spectra were recorded by means of UV/VIS spectrometer PU 8800 (Philips).

The pH measurements were performed using a combined glass electrode (Radelkis, Hungary).

The EPR spectra were recorded at a temperature of 290 K on a Bruker 200D spectrometer

coupled with an Aspect 2000 computer. The standard spectrometer settings were as follows: center field, 349 mT; sweep width, 8 mT; scan time, 20 s; microwave frequency, 9.72 GHz; microwave power, 10 mW; modulation, 0.05 mT; spectrometer gain from 10×10^4 to 4×10^5. The prepared TiO_2 suspensions ($c_{TiO_2} = 0.3$ g dm^{-3}) of AN1S and DMPO spin trap ($c_{DMPO} = 0.01$ M), were saturated by oxygen, then placed in a flat quartz cell, and irradiated directly in the TM cavity by the light of a 250-W medium-pressure mercury lamp (Applied Photophysics, England). Also here, a Pyrex filter was used to cut-off the radiation below 300 nm.

The concentration of sulfate ions in the samples was measured nephelometrically ($\lambda = 530$ nm) as $BaSO_4$.

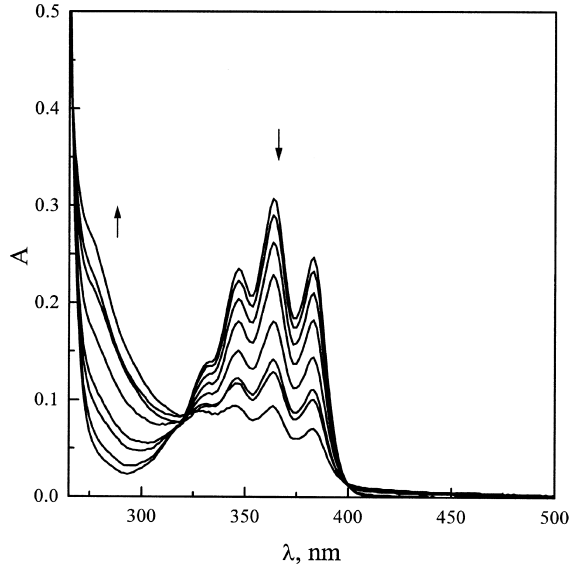

Fig. 1. Changes in UV/VIS spectra monitored during the irradiation of aqueous oxygen-saturated solution of AN1S. Initial AN1S concentration, $c_0 = 5 \times 10^{-5}$ mol dm^{-3}. Exposure: 0, 1, 3, 5, 10, 15, 20 and 30 min. Cell length: 1 cm.

3. Results and discussion

3.1. Phototransformation of AN1S in aqueous solutions

The effective formation of photogenerated charge carriers (electrons, holes) in TiO_2 P25 photocatalyst requires the ultra band gap irradiation below 400 nm [2,3]. Unfortunately, AN1S molecule absorbs significantly in the region of 300–400 nm (selected by the given experimental conditions) (Fig. 1). Therefore, at first it was necessary to investigate the photochemical transformations of AN1S in the TiO_2-free aqueous solutions. Fig. 1 represents the set of UV/VIS spectra obtained during irradiation of 5×10^{-5} M AN1S aqueous solutions. These spectra unambiguously demonstrate the decrease in the AN1S concentration during illumination. The decomposition of AN1S in the irradiated samples was precisely monitored by HPLC for the solutions with various initial concentrations of AN1S (Fig. 2). The obtained dependencies of AN1S concentration on the irradiation time (Fig. 2) may be described by the formal first-order kinetics, and the formal rate of AN1S disappearance, r, may be written as follows:

$$r = -\frac{dc}{dt_{exp}} = k_f c \quad (1)$$

$$c = c_0 \exp(-k_f t_{exp}) \quad (2)$$

where c is the actual AN1S concentration; t_{exp} is the irradiation time; k_f is the formal first-order rate constant; c_0 is the initial AN1S concentration.

The experimental data depicted in Fig. 2 were successfully fitted by the non-linear minimization procedure to the exponential function (Eq. (2)), and the values of the formal first-order rate constants were evaluated. At the very beginning of irradiation, the concentration of AN1S may be approximated to the initial concentration, c_0, as the concentrations of the degradation products are still negligible. Consequently, the formal initial rate of AN1S decomposition, r_0, can be defined as:

$$r_0 = k_f c_0 \quad (3)$$

Fig. 3 illustrates the dependence of the calculated formal initial rates of AN1S decomposition on the initial concentration of AN1S. We obtained excellent linear fit ($R^2 = 0.992$) in accordance with the Beer–Lambert law.

The mechanism of AN1S photodecomposition in the aqueous solutions is not fully explained yet. The photochemical desulfonation of anthracene-1-sulfonic acid, and the formation of anthracene was observed in strongly acidic solutions [26,27]. Competitive photodesulfonation and photodesulfonylation reactions were proposed for sodium arylsulfonates in aqueous media [28,29]. Previously, the formation of $SO_3^{\cdot -}$ radicals during photolysis of *p*-toluenesulfonate solutions was evidenced in our laboratory applying spin trapping technique [30]. On the other hand, in our EPR experiments using AN1S, $SO_3^{\cdot -}$ radicals were not observed by the irradiation of AN1S neither in the argon- nor oxygen-saturated aqueous solutions [24]. Instead, the intermediate radical product, AN-1-$SO_2^{\cdot}$, with limited stability was measured and, additionally, in the presence of oxygen the formation of hydroxyl radicals was monitored using DMPO spin trap [24]. We established previously the formation of anthraquinone-sulfonate by irradiation of AN1S in oxygenated aqueous solutions [24]. The ability of anthraquinone-sulfonates to activate oxygen and to generate $O_2^{\cdot -}$ and $OH^{\cdot}$ radicals is well described in the literature [31–34]. The hydroxyl radicals photogenerated in AN1S solutions play a dominant role in the destructive oxidation of anthracene or anthraquinone skeleton [22,35]. Unfortunately, we were not able to identify all AN1S photoproducts using HPLC. However, we unambiguously confirmed the formation of phthalic and salicylic acids, and we monitored their concentrations during irradiation (Fig. 4).

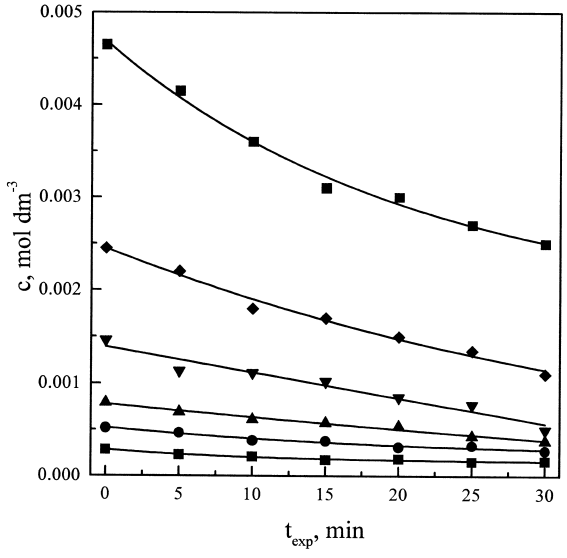

Fig. 2. The decrease of AN1S concentration during irradiation in solutions with different initial AN1S concentrations measured by HPLC.

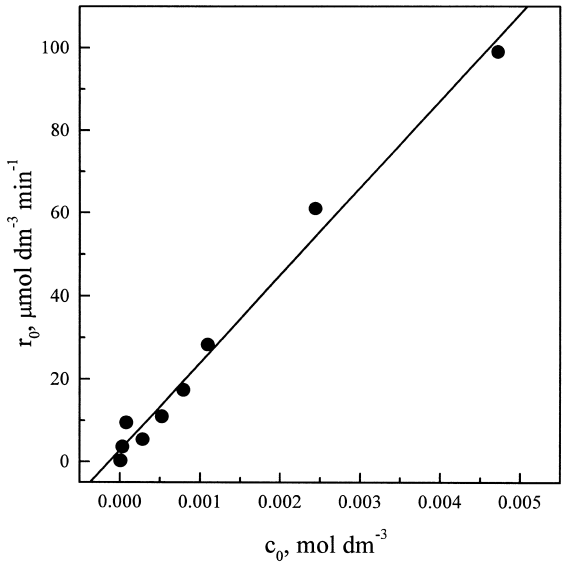

Fig. 3. Linear dependence of the formal initial rate of AN1S decomposition on the initial AN1S concentration evaluated for photoreaction in homogeneous oxygen-saturated aqueous solutions ($R^2 = 0.992$).

3.2. Photodegradation of AN1S in aqueous TiO_2 suspensions

In order to eliminate the contribution of direct AN1S phototransformation changing the initial substrate concentration, we performed our photocatalytic experiments in the large concentration range from 1×10^{-5} up to 3×10^{-3} M. The effective and very fast photocatalytic destruction of AN1S in TiO_2 suspensions was

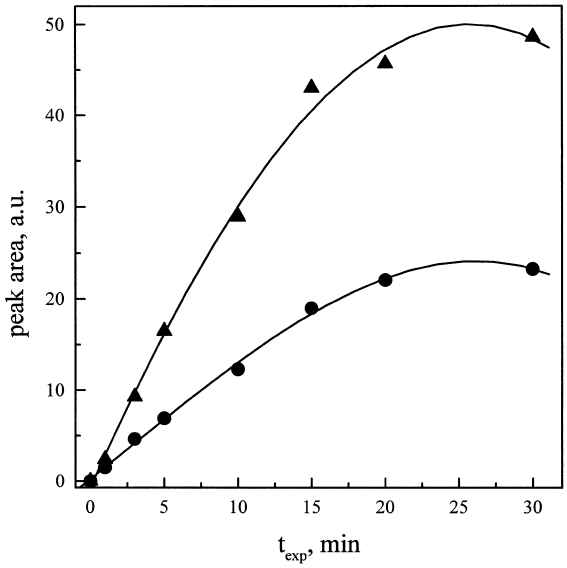

Fig. 4. HPLC peak area vs. irradiation time for phthalic acid (●) and salicylic acid (▲) measured during the illumination of aqueous oxygen-saturated solution of AN1S. Initial AN1S concentration $c_0 = 5\times10^{-5}$ mol dm^{-3}.

ascertained (Fig. 5). The experimental dependencies of AN1S concentration on the irradiation time were again fitted by the formal first-order kinetic model (Eq. (2)), and the formal initial rates, r_0, were evaluated. Fig. 6 represents the dependence of the formal initial rate of photodegradation vs. initial AN1S concentration. Assuming a self-ruling contribution of the photochemical and photocatalytic processes to the total AN1S decomposition rate, we attempted to separate the experimental data, as shown in Fig. 6. Certainly, the presence of TiO_2 significantly increases the formal initial photodegradation rate of AN1S due to the effective production of hydroxyl radicals in the irradiated oxygenated aqueous TiO_2 suspensions [19]. HPLC analysis of AN1S irradiated in TiO_2 suspensions proved main degradation products in the liquid phase; phthalic acid, salicylic acid and alizarin. Furthermore, the formation of these degradation products was unambiguously confirmed by abstract factor analysis [36,37] of the UV/VIS spectra set. This finding is in accordance with the photocatalytic degradation pathway proposed by Theurich et al. [22] for anthracene. Probably, the substitution on an-

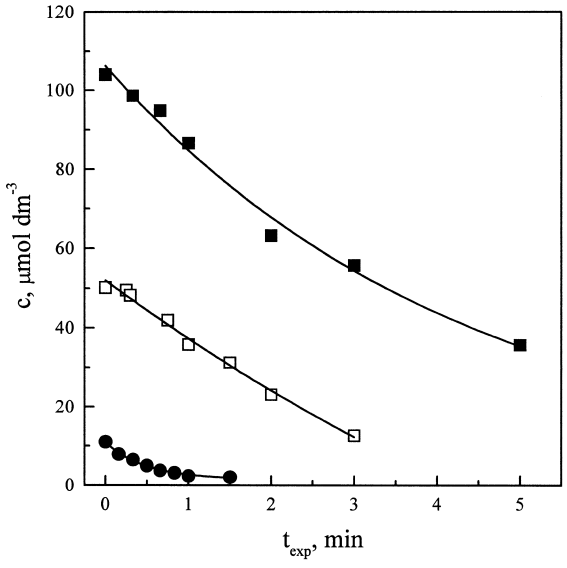

Fig. 5. The decrease of AN1S concentration during irradiation in oxygen-saturated TiO_2 suspensions with different initial AN1S concentrations measured by HPLC (TiO_2 concentration, $c_{TiO_2} = 1$ g dm^{-3}).

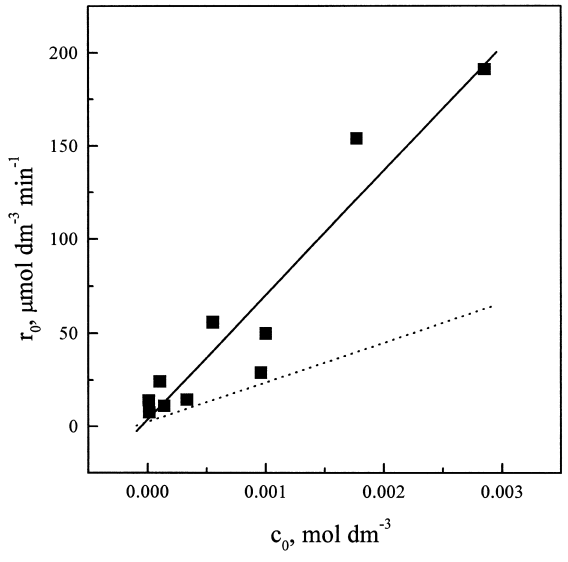

Fig. 6. Dependence of the formal initial rate of AN1S decomposition on the initial AN1S concentration evaluated for photocatalytic reaction in oxygen-saturated TiO_2 aqueous suspensions ($R^2 = 0.946$; TiO_2 concentration, $c_{TiO_2} = 1$ g dm^{-3}). The dashed line represents contribution of direct photochemical process evaluated in Fig. 3.

thracene skeleton has only inconsequential influence on the degradation mechanism initiated by hydroxyl radicals. Previously, it was evidenced that sulfonate group of arylsulfonates is during photocatalytic degradation in TiO_2 systems replaced by hydroxyl group [17,18]. Analogously, the concentration of SO_4^{2-} ions corresponding to 30% yield, was measured nephelometrically after 30 min of illumination for 0.001 M AN1S in titanium dioxide suspension ($c_{TiO_2} = 1$ g dm^{-3}) at 295 K.

The formal initial AN1S degradation rate measured in oxygen-saturated TiO_2 suspensions is dependent on the titanium dioxide concentration (Fig. 7). Here, we obtained the typical curve for initial rate vs. TiO_2 concentration, as published previously for other photocatalytic processes [16].

3.3. Effect of pH

The dependencies of formal initial rate of AN1S decomposition on pH values in homogeneous solutions, as well as heterogeneous TiO_2 suspensions are presented in Fig. 8. The observed variation of formal initial rate vs. solution pH in homogeneous systems in only small (Fig. 8). The shift of absorption bands in UV/VIS spectrum of AN1S caused by change of pH values was not detected. Consequently, the primary absorption of incident light by AN1S is not influenced. The increase of formal initial rate of AN1S degradation at pH = 12 is probably caused by acid–base equilibrium of photoproducts, or by alteration of hydroxyl radical reaction mechanism at high pH values as discussed below.

On the other hand, the pH values can significantly influence TiO_2 particle surface charge [6,7,38–41]. The ionization of hydroxyl groups on the TiO_2 surface depends on pH according to the following reactions:

$$TiOH + OH^- \leftrightarrow TiO^- + H_2O \quad (4)$$

$$TiOH + H^+ \leftrightarrow TiOH_2^+ \quad (5)$$

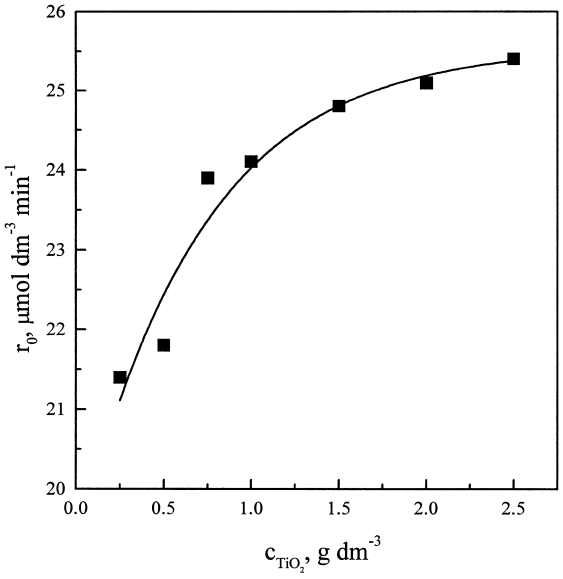

Fig. 7. Dependence of the formal initial rate of AN1S decomposition on TiO_2 concentration evaluated for photocatalytic reaction in oxygen-saturated TiO_2 aqueous suspensions (initial AN1S concentration, $c_0 = 0.001$ mol dm^{-3}).

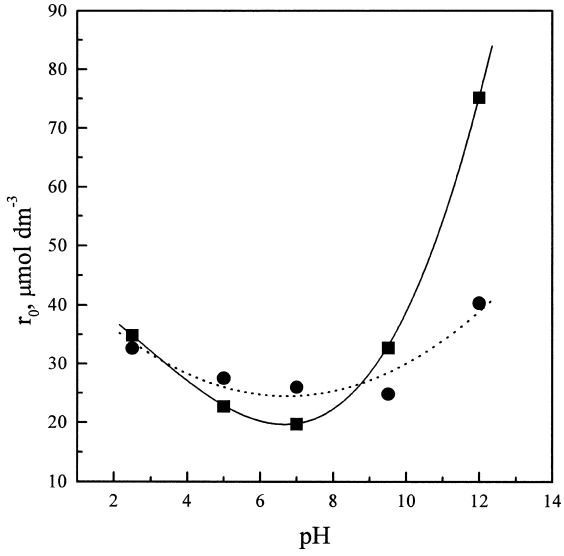

Fig. 8. Dependence of the formal initial rate of AN1S decomposition on pH value evaluated for photochemical reaction in solutions (●), and for photocatalytic reaction in TiO_2 aqueous suspensions (■). Initial AN1S concentration, $c_0 = 0.001$ mol dm^{-3}; TiO_2 concentration, $c_{TiO_2} = 1$ g dm^{-3}).

The zero zeta potential for the TiO_2 P25 Degussa sample was previously established at pH $= 6 \pm 0.5$ [19,39,41]. At pH < 6, the surface of TiO_2 particle is charged positively, while at pH > 6 the surface charge is negative [19].

Under given experimental conditions, the formal initial AN1S degradation rate reaches minimum at pH ~ 6 (Fig. 8), where the surface charge is zero. Therefore the adsorption of charged AN1S or photoproduced intermediates plays an significant role in the photocatalytic degradation mechanism. At first we proposed that positively charged surface enhance the adsorption of AN1S anions, and we expect the highest formal initial rates are possible at pH $<$ 6. However, the highest initial rate of AN1S degradation was monitored in TiO_2 suspensions at pH = 12. The analogous rate enhancements at pH > 12 was observed in the photocatalytic degradation of phenol in TiO_2 systems, and the possibility of formation different oxidizing species (oxide radical anion) was proposed, which provides an additional and/or alternative pathway of degradation [6]. In the photocatalytic degradation of anthracene it was pointed that the main reaction is probably the hydroxyl radical attack followed by the subsequent reaction with oxygen forming peroxyl radicals which eliminate superoxide radicals [22]. The essential role of superoxide radical-anion as an active species in the photocatalytic degradation of pollutants was shown by Amalric [42]. Therefore, it appears that the enhancement of formal initial AN1S degradation rate at pH > 9.5 reflect probably an additional pathway of degradation initiated by $O^{\cdot}$ or $O_2^{\cdot -}$ [6,42,43].

3.4. EPR spin trapping of hydroxyl radicals photogenerated in TiO_2 suspensions

As the hydroxyl radicals play an important role in the destruction of the anthracene skeleton, we completed our study with in situ EPR measurements of $OH^{\cdot}$ radicals using DMPO spin trap.

DMPO reacts with hydroxyl radicals forming $^{\cdot}$DMPO–OH adduct with characteristic splitting in EPR spectrum (for aqueous systems $a_H = a_N = 1.49$ mT [19]). The experimental spectrum of $^{\cdot}$DMPO–OH adduct measured in the irradiated oxygen-saturated TiO_2 suspensions containing AN1S, as well as its simulation ($g = 2.0058$, $a_H = a_N = 1.50$ mT), is depicted in Fig. 9. Previously, the EPR spin trapping technique using DMPO was successfully applied in the study of competitive reactions of organic substrates with hydroxyl radicals (Eqs. (6) and (7)), and the rate

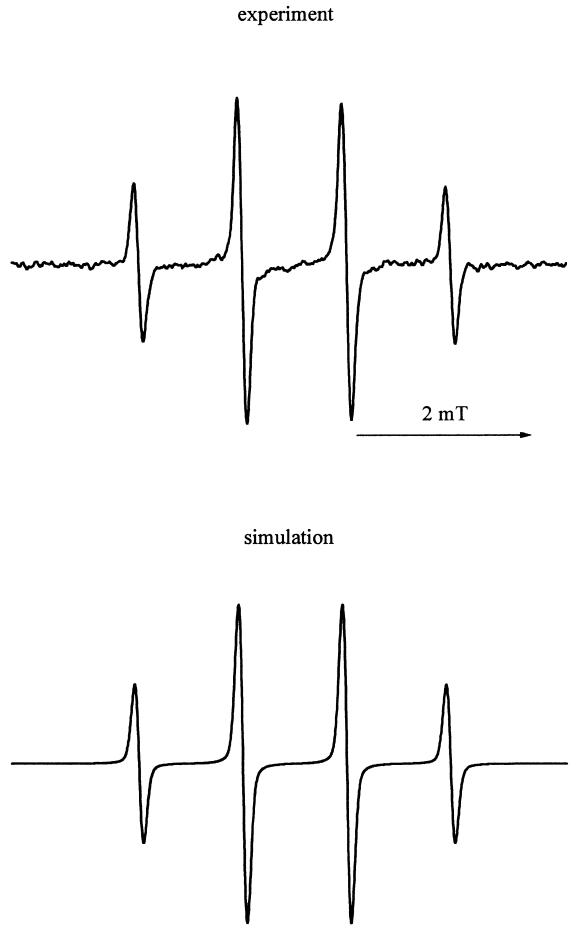

Fig. 9. Experimental and simulated EPR spectrum of hydroxyl radical generated and added to DMPO spin trap in the irradiated TiO_2 suspension of AN1S. Splitting constants: $a_H = a_N = 1.50$ mT, $g = 2.0058$. Initial concentration of DMPO, $c_{DMPO} = 0.01$ mol dm^{-3}; TiO_2 concentration, $c_{TiO_2} = 0.3$ g dm^{-3}; initial AN1S concentration, $c_0 = 1 \times 10^{-4}$ mol dm^{-3}.

constants for the reaction of ˙OH radicals with selected substrates were evaluated [19,44,45].

$$\text{DMPO} + {}^{\cdot}\text{OH} \rightarrow {}^{\cdot}\text{DMPO–OH} \quad \text{EPR signal} \tag{6}$$

$$\text{Substrate} + {}^{\cdot}\text{OH} \rightarrow \text{products} \quad \text{EPR silent} \tag{7}$$

In our study, we monitored the competitive reaction of ˙OH radicals between AN1S and DMPO in the TiO_2 suspensions with various concentrations of AN1S at constant concentrations of DMPO and TiO_2 ($c_{DMPO} = 0.01$ mol dm^{-3}, $c_{TiO_2} = 0.3$ g dm^{-3}). The increase in concentration of AN1S which reacts with hydroxyl radicals, inhibited the formation of ˙DMPO–OH adduct and, consequently, the relative intensity of its EPR signal decreased. During in situ measurements using continuous irradiation, the relative EPR intensity of ˙DMPO–OH radical reaches maximum at 80 s of irradiation and then decreases. This decrease is probably caused by the repeated attack of ˙OH radical on DMPO, which results in the spin trap destruction.

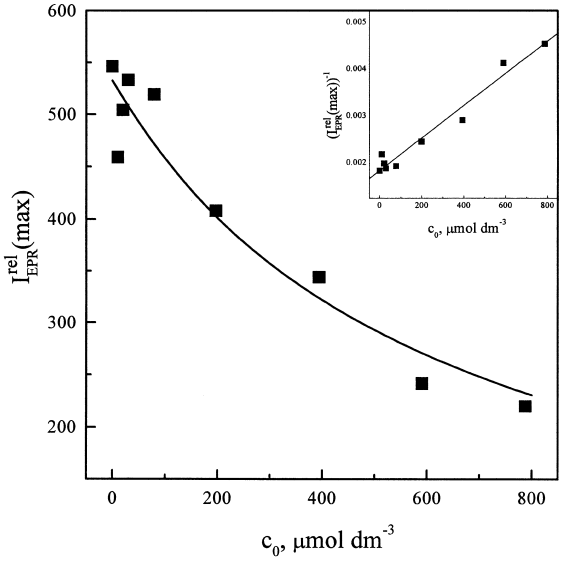

Fig. 10. Dependence of maximal relative intensity of EPR signal of ˙DMPO–OH adduct (measured after 80 s of irradiation) vs. initial AN1S concentration. Inset: Linear dependence of $(I^{rel}_{EPR}(max)^{-1}$ on the initial AN1S concentration ($R^2 = 0.996$). Initial concentration of DMPO, $c_{DMPO} = 0.01$ mol dm^{-3}; TiO_2 concentration, $c_{TiO_2} = 0.3$ g dm^{-3}.

The maximal relative EPR intensity of ˙DMPO–OH adduct achieved in systems with various AN1S concentrations can be chosen for the evaluation of concentration dependence (Fig. 10) as was described previously [46]. Thus, at a defined irradiation time, $t_{exp} = 80$ s, a linear dependence of the reciprocal values of maximal relative EPR intensity of ˙DMPO–OH signal, $I^{rel}_{EPR}(max)$, on the various initial concentration of AN1S, c_0, was obtained (inset in Fig. 10). The excellent linear fit achieved here ($R^2 = 0.996$, inset Fig. 10) confirmed the competitive reaction of ˙OH radicals between DMPO spin trap and AN1S substrate.

4. Conclusions

The decomposition of AN1S in oxygen-saturated aqueous solutions and TiO_2 suspensions by irradiation ($\lambda > 300$ nm) follows the formal first-order kinetics. The presence of titanium dioxide significantly enhances the formal initial photodegradation rate of AN1S. The formation of phthalic and salicylic acids was monitored by HPLC in both homogeneous and heterogeneous photosystems. Additionally, the production of alizarin during irradiation in the presence of TiO_2 was confirmed. The photogenerated hydroxyl radicals play an important role in the degradation mechanism of polyaromatic skeleton. In situ EPR spin trapping experiments in oxygen-saturated aqueous TiO_2 suspensions of AN1S confirmed the competitive reaction of hydroxyl radicals between DMPO spin trap and AN1S.

Acknowledgements

We thank the Slovak Grant Agency (projects VEGA 1/4206/97 and 1/6156/99) for the financial support.

References

[1] O. Legrini, E. Oliveros, A.M. Braun, Chem. Rev. 93 (1993) 671.
[2] M.R. Hoffmann, S.T. Martin, W. Choi, D.W. Bahnemann, Chem. Rev. 95 (1995) 69.
[3] A. Mills, S. le Hunte, J. Photochem. Photobiol., A 108 (1997) 1.
[4] R.W. Matthews, J. Phys. Chem. 91 (1987) 3328.
[5] R.W. Matthews, J. Catal. 113 (1988) 549.
[6] K.E. O'Shea, C. Cardona, J. Photochem. Photobiol., A 91 (1995) 67.
[7] L. Zang, C.-Y. Liu, X.-M. Ren, J. Chem. Soc., Faraday Trans. 91 (1995) 917.
[8] H. Hidaka, H. Kubota, M. Grätzel, N. Serpone, E. Pelizzetti, Nouv. J. Chim. 9 (1985) 67.
[9] J. Zhao, H. Hidaka, A. Takamura, E. Pelizzetti, N. Serpone, Langmuir 9 (1993) 1646.
[10] J. Zhao, H. Oota, H. Hidaka, E. Pelizzetti, N. Serpone, J. Photochem. Photobiol., A 69 (1992) 251.
[11] H. Hidaka, Proc. Indian Acad. Sci. (Chem. Sci.) 110 (1998) 215.
[12] L. Muszkat, L. Bir, L. Feigelson, J. Photochem. Photobiol., A 87 (1995) 85.
[13] C. Domínguez, J. García, M.A. Pedraz, A. Torres, M.A. Galán, Catal. Today 40 (1998) 85.
[14] R. Doong, W.-H. Chang, J. Photochem. Photobiol., A 107 (1997) 239.
[15] C. Bouquet-Somrani, A. Finiels, P. Graffin, J.-L. Olivé, Appl. Catal., B 8 (1996) 101.
[16] R. Terzian, N. Serpone, J. Photochem. Photobiol., A 89 (1995) 163.
[17] V. Brezová, M. Jankovičová, M. Soldán, A. Blažková, M. Reháková, I. Šurina, M. Čeppan, B. Havlínová, J. Photochem. Photobiol., A 83 (1994) 69.
[18] B. Sangchakr, T. Hisanaga, K. Tanaka, J. Photochem. Photobiol., A 85 (1995) 187.
[19] V. Brezová, A. Staško, S. Biskupič, A. Blažková, B. Havlínová, J. Phys. Chem. 98 (1994) 8977.
[20] E. Pramauro, A.B. Prevot, M. Vincenti, R. Gamberini, Chemosphere 36 (1998) 1523.
[21] C. Guillard, H. Delprat, C. Hoang-Van, P. Pichat, J. Atmos. Chem. 16 (1993) 47.
[22] J. Theurich, D.W. Bahnemann, R. Vogel, F.E. Ehamed, G. Alhakimi, I. Rajab, Res. Chem. Intermed. 23 (1997) 247.
[23] M. Okawara, T. Kitao, T. Hirashima, M. Matsuoka, Organic Colorants, Elsevier, 1999.
[24] A. Staško, A. Blažková, V. Brezová, M. Breza, L. Lapčík, L. Lapčík Jr., J. Photochem. Photobiol., A 76 (1993) 159.
[25] J.F. Rabek, Experimental Methods in Photochemistry, Photophysics, Wiley, New York, 1985, p. 945.
[26] A.V. El'tsov, O.P. Studzinskii, N.I. Rtishchev, A.V. Devekki, M.V. Sendyurev, J. Org. Chem. USSR 10 (1974) 2567.
[27] O.P. Studzinskii, N.I. Rtishchev, N.N. Kravchenko, A.V. El'tsov, J. Org. Chem. USSR 11 (1975) 386.
[28] Y. Izawa, N. Suzuki, A. Inoue, K. Ito, T. Ito, J. Org. Chem. 44 (1979) 4581.
[29] A.M. Braun, M.-T. Maurette, E. Oliveros, Photochemical Technology, Wiley, Chichester, 1991, p. 397.
[30] V. Brezová, A. Staško, S. Biskupič, J. Photochem. Photobiol., A 71 (1993) 229.
[31] K. Lang, D.M. Wagnerová, P. Stopka, J. Photochem. Photobiol., A 67 (1992) 187.
[32] K.P. Clark, H.I. Stonehill, J. Chem. Soc., Faraday Trans. 1 68 (1972) 1676.
[33] I. Loeff, A. Treinin, H. Linschitz, J. Phys. Chem. 87 (1983) 2536.
[34] G.O. Phillips, N.W. Worthington, J.F. McKellar, R.R. Sharpe, J. Chem. Soc. (1969) 767.
[35] J. Kiwi, C. Pulgarin, P. Peringer, M. Grätzel, Appl. Catal., B 3 (1993) 85.
[36] E.R. Malinowski, in: H.L.C. Meuzelaar, T.L. Isenhour (Eds.), Computer-Enhanced Analytical Spectroscopy, Plenum, New York, 1987.
[37] P. Pelikán, M. Čeppan, M. Liška, Applications of Numerical Methods in Molecular Spectroscopy, Chap. 3, CRC Press, Boca Raton, 1994, p. 71.
[38] L.-C. Chen, T.-C. Chou, J. Mol. Catal. 85 (1993) 201.
[39] M.A. Fox, M.T. Dulay, J. Photochem. Photobiol., A 98 (1996) 91.
[40] D.H. Kim, M.A. Anderson, J. Photochem. Photobiol., A 94 (1996) 221.
[41] L. Zang, P. Qu, J. Zhao, T. Shen, H. Hidaka, J. Mol. Catal. A: Chem. 120 (1997) 235.
[42] L. Amalric, C. Guillard, P. Pichat, Res. Chem. Intermed. 20 (1994) 579.
[43] D.E. Cabelli, in: Z.B. Alfasi (Ed.), Peroxyl Radicals, Chap. 13, Wiley, New York, 1997, p. 407.
[44] J. Kochany, J.R. Bolton, J. Phys. Chem. 95 (1991) 5116.
[45] R. Morelli, I.R. Bellobono, C.M. Chiodaroli, S. Alborghetti, J. Photochem. Photobiol., A 112 (1998) 271.
[46] V. Brezová, A. Staško, J. Catal. 147 (1994) 156.